Genomics 103 (2014) 337–348

Contents lists available at ScienceDirect

Genomics

journal homepage: www.elsevier.com/locate/ygeno

Transcriptome analysis of human primary endothelial cells (HUVEC) from umbilical cords of gestational diabetic mothers reveals candidate sites for an epigenetic modulation of specific gene expression

R. Ambra [a,*], S. Manca [a], M.C. Palumbo [a,b], G. Leoni [a], L. Natarelli [a], A. De Marco [d], A. Consoli [d], A. Pandolfi [c], F. Virgili [a]

[a] Food and Nutrition Center of the Agricultural Research Council - CRA-NUT, via Ardeatina 546, 00178 Rome, Italy
[b] Institute for Computing Applications M. Picone, National Research Council of Italy (CNR), via dei Taurini 19, 00185 Rome, Italy
[c] Department of Experimental and Clinical Sciences, University G. d'Annunzio, Aging Research Center, Center of Excellence for Aging, G. d'Annunzio University Foundation, Chieti-Pescara, Italy
[d] Department of Medicine and Aging Sciences, University G. d'Annunzio, Aging Research Center, Center of Excellence for Aging, G. d'Annunzio University Foundation, Chieti-Pescara, Italy

ARTICLE INFO

Article history:
Received 3 October 2013
Accepted 5 March 2014
Available online 22 March 2014

Keywords:
Hyperglycemia
Gestational diabetes
HUVEC
Transcriptome
Epigenetic

ABSTRACT

Within the complex pathological picture associated to diabetes, high glucose (HG) has "*per se*" effects on cells and tissues that involve epigenetic reprogramming of gene expression. In fetal tissues, epigenetic changes occur genome-wide and are believed to induce specific long term effects. Human umbilical vein endothelial cells (HUVEC) obtained at delivery from gestational diabetic women were used to study the transcriptomic effects of chronic hyperglycemia in fetal vascular cells using Affymetrix microarrays. In spite of the small number of samples analyzed (n = 6), genes related to insulin sensing and extracellular matrix reorganization were found significantly affected by HG. Quantitative PCR analysis of gene promoters identified a significant differential DNA methylation in TGFB2. Use of Ea.hy926 endothelial cells confirms data on HUVEC. Our study corroborates recent evidences suggesting that epigenetic reprogramming of gene expression occurs with persistent HG and provides a background for future investigations addressing genomic consequences of chronic HG.

1. Introduction

Sustained hyperglycemia (HG) has important effects at different levels. At the cellular level, HG imposes a significant derangement of normal metabolic homeostasis [1]. In tissues, long term HG is responsible for a large number of diabetes side effects ranging, amongst others, from vascular to immune system failure [2,3]. Gestational diabetes (GD) is a specific form of diabetes affecting about 8% of pregnant women and caused by a relative failure of pancreatic β-cells to produce extra insulin necessary to overcome the physiological increase of insulin resistance taking place throughout pregnancy [4]. GD usually reverses after delivery, but altered glucose homeostasis harms the mother and can lead to health consequences in the fetus. In fact, untreated GD is associated to a spectrum of neonatal pathologies, ranging from overweight at delivery, hypoglycemia, macrosomia, cardiac dysfunction and congenital malformations [5]. In spite of this wide spectrum of complications, no specific genetic factors associated to GD have been identified yet [6]. However, available reports, together with the observation that GD displays in daughters of affected mothers an incidence higher than one would expect from a canonical Mendelian inheritance, strongly support the hypothesis of an epigenetic basis for GD [7].

Epigenetic reprogramming of genes is a crucial event in particular during fetal development, where genome-wide epigenetic changes occur. In fact, recent observations indicate that diabetes is associated to epigenetic reprogramming of gene expression [8], possibly due to HG that triggers specific molecular effects during prenatal growth then fixed in the fetus genome. In order to test this hypothesis, we have analyzed the transcriptome of human umbilical vein endothelial cells (HUVEC) obtained from the vein of umbilical cords collected from GD patients, and compared to control cells obtained from healthy donors. These cells are an expedient *ex vivo* model for the study of the molecular consequences of chronic HG. In fact, it is well known that primary endothelial cells in culture have a special sensitivity to high glucose and cannot be cultured for more than a few passages without losing their specific characteristics.

Our data indicate that a significant up-regulation of several genes encoding for growth factors linked to insulin sensing and extracellular matrix (ECM) occurs in GD-HUVEC cells. Microarray data, confirmed by RT-qPCR, strongly suggest that GD-HUVEC faithfully recapitulate several molecular changes previously reported in GD patients and

* Corresponding author.
E-mail address: roberto.ambra@entecra.it (R. Ambra).

http://dx.doi.org/10.1016/j.ygeno.2014.03.003
0888-7543/

associated to HG. Moreover, qPCR analysis of genomic DNA digested with methylation-dependent or sensitive restriction enzymes was used to identify differential promoter methylation in a subset of genes. Differential expression of transforming growth factor β 2 (TGFB2), found in GD-HUVEC, correlates with differential promoter methylation, suggesting an important role in the set up and propagation of a "glycemic memory" in endothelial cells. Finally, utilizing the stable endothelial cell line Ea.hy926, we have confirmed the existence of an HG-driven methylation mechanism leading to an epigenetic modulation of TGFB2 expression.

2. Materials and methods

2.1. Ethics statement

Umbilical cords were obtained from randomly selected healthy and gestational diabetic mothers delivering at the Pescara Town Hospital (Italy). All procedures were in agreement with the ethical standards of the Institutional Committee on Human Experimentation ("University G. d'Annunzio Ethics Committee review board", Reference Number: 1879/09COET) and with the Declaration of Helsinki Principles. After approval of the protocol by the Institutional Review Board, a signed informed consent form was obtained from each participating subject.

2.2. HUVEC primary endothelial cells

Primary cultures of endothelial cells (HUVEC) were set after enzymatic digestion of endothelial tissue of umbilical cord vein as previously reported [9]. Umbilical cords were collected immediately after delivery (39 to 41 weeks), from 3 Caucasian GD women (GD diagnosed not later than 28th gestational week, GW, and fully recovered after delivery) and from 3 Caucasian nondiabetic (C) women randomly selected matching for age (35.6 ± 4.0 and 34.4 ± 4.5, respectively) and pre-gestational weight (kg, 62.1 ± 13.7 and 67.9 ± 29.3). Basic anthropometric parameters did not differ significantly between the groups: height (mt) 1.66 ± 0.04 (C) and 1.62 ± 0.09 (GD) and pre-gestational body mass index: 22.5 ± 3.7 (C) and 25.5 ± 2.4 (GD). Routine and clinical analyses were similar in both GD and control subjects (data not shown) with the exception of the biochemical fasting glycemia (4.33 ± 0.66 and 5.16 ± 0.48 mM, in control and GD group respectively). Nucleic acids were extracted from HUVEC strains after 4 passages in normal glucose (5.5 mM) M199 endothelial growth medium (BioWhittaker) supplemented with 20% FBS, 10 μg/mL heparin, and 50 μg/mL ECGF (Sigma), in order to discard genes whose expression should not depend on epigenetic changes during gestational growth.

2.3. Ea.hy926 cells and HG treatment

The stabilized cell line Ea.hy926 is constituted of endothelial cells derived from the fusion of HUVEC with the human lung carcinoma cell line A549 [10]. Cells were cultured in 5.5 mM glucose DMEM (EuroClone) supplemented with 10% FCS, 100 IU/mL penicillin, 0.1 mg/mL streptavidin, 2 mM L-glutamine and 2% HAT (hypoxanthine, amnopterin, thymidine). HG condition was obtained treating cells for 24 h in 25.5 mM glucose. For the normal-glucose recovery condition, cells were synchronized by starvation using 0.1% FBS media, starting from 12 h from seeding, in order to avoid artifacts in the quantification of methylation due to DNA duplication, which is especially relevant in non-synchronized cell populations.

2.4. RNA extraction and cDNA microarray experiment

Total RNA from GD-HUVEC and HUVEC was extracted using RNeasy Plus Mini Kit (Qiagen, Hilden, Germany), according to the manufacturer's instructions. Isolated RNA samples were sent to ServiceXS BV (Leiden, The Netherlands) to be processed according to Affymetrix protocols. Briefly, total RNA was labeled with the Affymetrix Eukaryotic One-Cycle Target Labeling and Control reagents to generate biotin-labeled anti-sense cRNA. Labeled cRNAs were hybridized on custom Affymetrix chips (NuGO_Hs1a520180) containing 23,941 probesets including 71 controls (for details http://www.ebi.ac.uk/arrayexpress/arrays/A-AFFY-111/). Graphic files obtained following chip hybridization were analyzed using the R package oneChannelGUI. Raw signals were normalized utilizing the GCRMA algorithm. The list of differentially expressed genes was obtained applying a linear and moderated T-statistic model that implements empirical Bayes regularization of standard errors. According to the statistical test we selected only genes with a Benjamini–Hochberg corrected p-value < 0.05 and a Log_2 ratio (FC) between mean values of expression of GD-HUVEC vs control cells greater than 1 or below −1. According to the microarray analysis a total number of 127 genes resulted in being significantly modulated in GD-HUVEC compared to control cells (see the Result section). Among those, 29 have a FC greater or lower than ±2, while 55 genes have a FC greater or lower than ±1.5. Because of the small number of samples analyzed, we thought of calculating the probability to detect false positive differentially expressed genes, estimating the statistical power of the microarray experiment at different thresholds of FC with the R package "size-power" [11]. Statistical power of genes above the ±2 FC threshold was 0.95. Genes below the threshold of ±1.5 had a power of 0.70 and those with a threshold of ±1 showed a 0.30 power value. As the functional analysis of the BP enrichment performed with genes from every threshold yielded similar results, annotation and data-mining were carried out with the complete list of genes, *i.e.* those produced according to the ±1 FC threshold (see Results).

2.5. RT-qPCR

Total RNA was extracted from HUVEC and Ea.hy926 cells using RNAeasy Plus Mini kit (Qiagen) according to the manufacturer's protocol. Purity, integrity and concentration were analyzed using the Agilent 2100 Bioanalyzer (Agilent Technologies). RNA was reverse transcribed and amplified using the Power SYBR Green RNA-to-CT 1-Step Kit (Life Technologies) according to manufacturer's instructions and applying the following thermal protocol: reverse transcription for 30 min at 48 °C; Taq activation for 10 min at 95 °C; 40 cycles of denaturation for 15 s at 95 °C and annealing/extension for 1 min at 60 °C. Finally, melting curve analysis was performed in order to verify the proper product amplification. Optimal input RNA concentration for each gene was chosen using standard curve analysis of a pool of samples or treatments. Ribosomal protein RPS9 was selected as an internal standard. Primer sequences are listed in Table 2. Measurements were performed in technical triplicate and repeated at least three separate times. Data in figures are expressed in Log_2 in order to provide symmetrical distribution of gene expression effects. All data are expressed as the ratio to the reference gene RPS9. Statistical significance was determined by unpaired Student's *t* test.

2.6. DNA extraction and qPCR analysis of promoter methylation

Genomic DNA was extracted using Qiagen Puregene Core Kit A according to the manufacturer's protocol and quantified using NanoDrop 1000 Spectrophotometer (Thermo Fisher Scientific). CpG island DNA methylation of individual genes was analyzed using the EpiTect Methyl qPCR Assay (Qiagen). The method, referred as "qAMP", is based on the detection of DNA remaining after cleavage with methylation-sensitive and/or methylation-dependent restriction enzymes. This method has been already reported to provide accurate and reproducible results without the requirement for sodium bisulfite treatment of DNA [12].

After digestion of unmethylated and methylated DNAs by methylation-sensitive and methylation-dependent restriction enzymes, residual DNA was quantified by qPCR using primers flanking the promoter region of interest. The relative fractions of hypermethylated (HM) and

unmethylated (UM) and intermediately methylated (IM) DNAs were subsequently determined by comparing the amount in each digest with a control untreated sample. The reaction mix was prepared according to manufacturer's instructions: briefly, four 50 ng of genomic DNA samples were digested at 37 °C for 16 h either with methylation-sensitive, methylation-dependent, mock or both restriction enzymes. Reactions were blocked by heat-inactivation at 65 °C for 20 min and PCR performed applying the following thermal protocol: 95 °C for 10 min; 3 cycles at 99 °C for 30 s and 72° for 1 min; 40 cycles at 97 °C for 15 s and 72 °C for 1 min. Ct values were used to calculate the percentage of HM, UM and IM DNAs using the datasheet provided at http://www.sabiosciences.com/dna_methylation_data_analysis1.php (*Individual EpiTect Methyl qPCR Assay*).

3. Results

3.1. Microarray analysis and annotation

The microarray analysis identified 127 genes differentially expressed in GD-HUVEC in comparison to HUVEC control cells obtained from non-diabetic mothers. The data discussed in this publication have been deposited in NCBI's Gene Expression Omnibus [13] and are accessible through GEO Series accession number GSE49524 (http://www.ncbi.nlm.nih.gov/geo/query/acc.cgi?acc=GSE49524). Statistical enrichment of specific biological processes, cellular compartments and molecular functions annotated in Gene Ontology (GO http://www.geneontology.org/) was assessed by the "clustering tool" included in the DAVID server (http://david.abcc.ncifcrf.gov/). For each GO category cluster provided by DAVID, a representative category was selected having the lowest p-value, corrected using the Benjamini–Hockberg method. Only non-redundant categories having a p-value lower than 0.05 were considered significant. 59 (47%) out of 127 differentially expressed genes were clustered into 7 main GO categories of Biological Processes (BP). Namely: organ development (GO: 0048513), anatomical structure morphogenesis (GO: 0009653), regulation of cell differentiation (GO: 0045595), response to external stimulus (GO: 000009605), cell communication (GO: 000007154), positive regulation of biological process (GO: 0048518) and regulation of immune response (GO: 0050776) (Fig. 1a). 27 genes (about 21% of the total) over represent the extracellular region part category (GO: 0044421), belonging to the cellular component (CC) GO ontology (Fig. 1a). No significant categories belonging to the molecular function (MF) ontology were found. Pathways analysis of differentially expressed genes strongly highlights the up-regulation of genes involved in organ development in GD-HUVEC. Some of them specifically encode for growth factors (BDNF, FST, TGFB2), protein constituents of the extra cellular matrix (COL1A1, COL3A1, FBN1, FBN2,

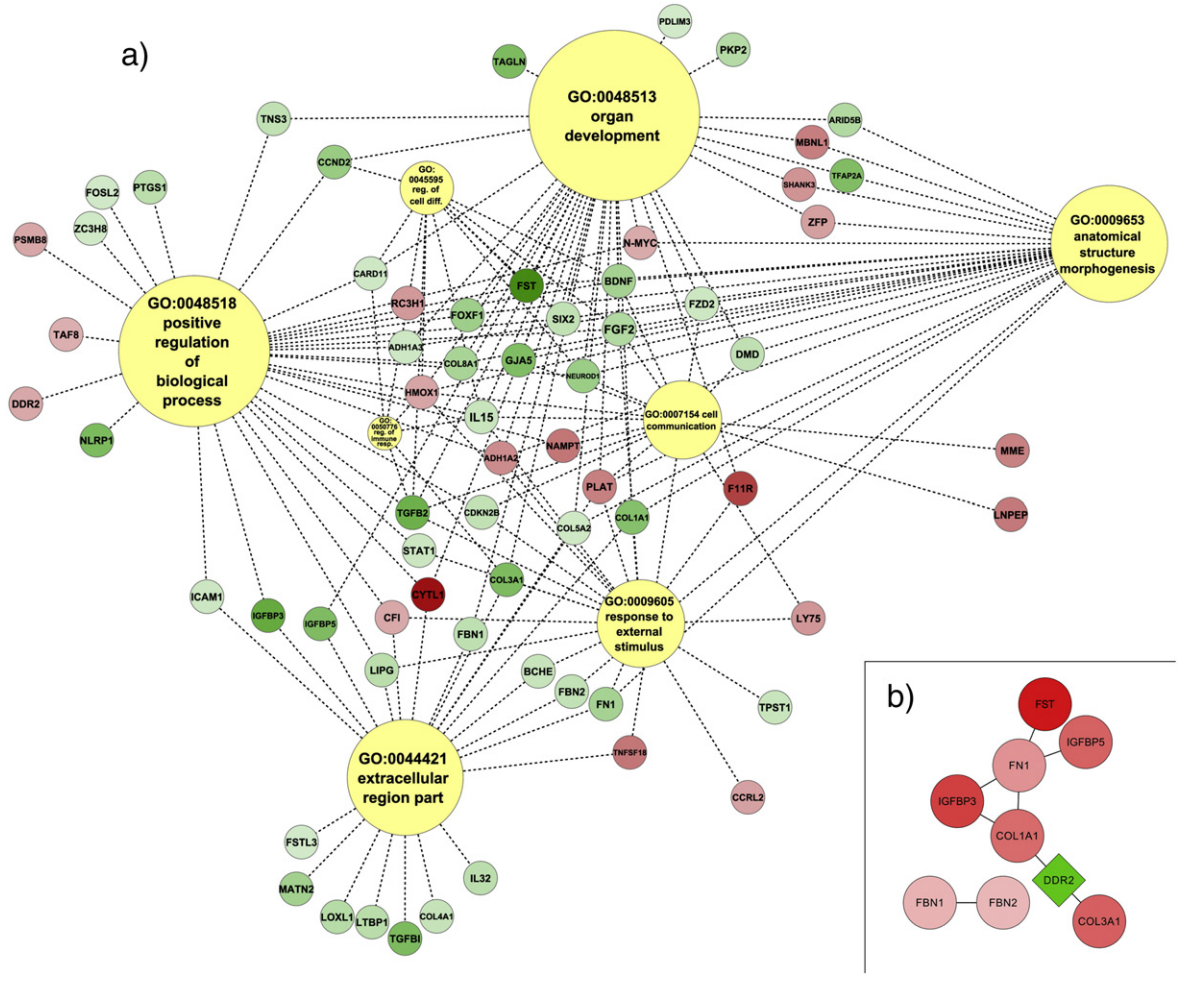

Fig. 1. (a) — Gene ontology. Representation (white nodes) of the biological processes and cellular component highlighted by the enrichment analysis. Each GO term is connected to its modulated genes (green nodes: up-regulated genes; red nodes: down-regulated genes). The size of the GO terms is proportional to the number of modulated genes. The topological position of genes in the network is determined by the number of connections and therefore by the number of GO terms in which the gene is involved. (b) — Directly connected genes. The search for direct relationship between modulated genes produced a very low relational graph, and made of only 9 genes: FBN1, FBN2, COL1A1, COL3A1, DDR2, IGFBP3, IGFBP5, FN1 and FST. Green nodes: up-regulated genes; red nodes: down-regulated genes. The intensity of color is proportional to gene regulation level.

Table 1
Abbreviations of terms depicted in networks.

Terms	Descriptions
Act	Activin, inhibin beta E chain
AKT	Protein kinase B alpha
ADH1A2	Aldehyde dehydrogenase 1 family, member A2
ADH1A3	Aldehyde dehydrogenase 1 family, member A3
Ang	Angiopoietins
ARID5B	AT rich interactive domain 5B (MRF1-like)
bCas	Beta casein
BCHE	Butyrylcholinesterase
BDNF	Brain-derived neurotrophic factor
C/EBP	CCAAT/enhancer binding protein (C/EBP), beta
CARD11	Caspase recruitment domain family, member 11
CCND2	Cyclin D2
CCRL2	Chemokine (C–C motif) receptor-like 2
CDKN2B	Cyclin-dependent kinase inhibitor 2B (p15)
CFI	Complement factor I
C-MYC	V-myc myelocytomatosis viral oncogene homolog
COL1A1	Collagen, type I, alpha 1
COL3A1	Collagen, type III, alpha 1
COL4A1	Collagen, type IV, alpha 1
COL5A2	Collagen, type V, alpha 2
COL8A1	Collagen, type VIII, alpha 1
CYTL1	Cytokine-like 1
CytR	Cytokine R
CytR-J	Cytokine R and JAK2 complex
DDR2	Discoidin domain receptor tyrosine kinase 2
DMD	Dystrophin
EGF	Epidermal growth factor
EGFR	Epidermal growth factor receptor
F11R	F11 receptor
FBN1	Fibrillin 1
FBN2	Fibrillin 2
FGF2	Fibroblast growth factor 2
FGF2R	Fibroblast growth factor receptor 2
FN1	Fibronectin 1
FOSL2	FOS-like antigen 2
FOXF1	Forkhead box F1
FOXO1	Forkhead box O1
FST	Follistatin
FSTL3	Follistatin-like 3
FZD2	Frizzled family receptor 2
GH1	Growth hormone 1
GHR	Growth hormone receptor
GJA5	Gap junction protein, alpha 5, 40 kDa
GLUT4	Glucose transporter type 4
GRB2	Growth factor receptor-bound protein 2
HMOX1	Heme oxygenase (decycling) 1
ICAM1	Intercellular adhesion molecule 1
IGF1,2	Insulin-like growth factors 1 and 2
IGF1R	Insulin-like growth factor 1 receptor
IGFBP3	Insulin-like growth factor binding protein 3
IGFBP5	Insulin-like growth factor binding protein 5
IkB	Inhibitor of kappa B
IL15	Interleukin 15
IL32	Interleukin 32
INS	Insulin
IR	Insulin receptor
IRS1	Insulin receptor substrates 1 and 2
ITG2	Integrin, beta 2 and alpha L, complex
JAK2	Janus kinase 2
LIPG	Lipase, endothelial
LNPEP	Leucyl/cystinyl aminopeptidase
LOXL1	Lysyl oxidase-like 1
LTBP1	Latent TGFB binding protein 1
LY75	Lymphocyte antigen 75
MATN2	Matrilin 2
MBNL1	Muscleblind-like splicing regulator 1
MIZ1	Zinc finger, MIZ-type containing 1
MME	Membrane metallo-endopeptidase
MMP	Matrix metallopeptidase
mTOR	Mechanistic target of rapamycin
NAMPT	Nicotinamide phosphoribosyltransferase
NDRG1	N-myc downstream regulated 1
NEUROD1	Neuronal differentiation 1
NF-κb	Nuclear factor of kappa B
NLRP1	NLR family, pyrin domain containing 1
NMI	N-myc (and STAT) interactor
N-MYC	V-myc myelocytomatosis viral related oncogene
p21	Cyclin-dependent kinase inhibitor 1A
p300	E1A binding protein p300
p53	Tumor protein p53
PDGFB	Platelet-derived GF beta polypeptide
PDGFbR	Platelet-derived GF receptor, beta polypep.
PDLIM3	PDZ and LIM domain 3
PI3K	Phosphatidylinositol-4,5-bisphosphate 3-kinase
PKP2	Plakophilin 2
Plas	Plasmin
PLAT	Plasminogen activator, tissue
PLAU	Plasminogen activator, urokinase
PLG	Plasminogen
PSMB8	Proteasome subunit, beta type, 8
PTGS1	Prostaglandin-endoperoxide synthase 1
RC3H1	Ring finger and CCCH-type domains 1
RNP	Heterogeneous nuclear ribonucleoproteins H
RPS9	Ribosomal protein S9
SERP1	Plasminogen activator inhibitor type 1
SHANK3	SH3 and multiple ankyrin repeat domains 3
SHC1	SHC transforming protein 1
SIRT1	Sirtuin 1
SIX2	SIX homeobox 2
SMAD	Small mother against decapentaplegic
SOS	SOS–Ras–Raf–MEK–ERK pathway
SP1	Sp1 transcription factor
STAT1	Signal transducer and activator of transcription
TAF8	RNA pol II TBP-associated factor
TAGLN	Transgelin
TFAP2A	Transcription factor AP-2 alpha
TGFB2	Transforming growth factor, beta 2
TGFBR	Transforming growth factor, beta receptor
TNF-a	Tumor necrosis factor
TNFR1,2	TNF receptor superfamily, members 1A and 1B
TNFSF18	TNF (ligand) superfamily, member 18
TNS3	Tensin 3
TPST1	Tyrosylprotein sulfotransferase 1
TRADD	TNFRSF1A-associated *via* death domain
TRAF2	TNF receptor-associated factor 2
TrkB	Neurotrophic tyrosine kinase, receptor, type 2
ZC3H8	Zinc finger CCCH-type containing 8
ZFP36L1	Zinc finger protein 36, C3H type-like 1

Approved gene symbols for the following genes are shown in parentheses: Act (INHBE), ADH1A2 (ALDH1A2), ADH1A3 (ALDH1A3), bCas (CSN2), C/EBP (CEBPB), C-MYC (MYC), FGF2R (FGFR2), IR (INSR), N-MYC (MYCN), PDGFbR (PDGFRB), Plas (PLG), TNF-a (TNF), TrkB (NTRK2).

FN1) and factors stabilizing insulin-like growth factors (IGFBP3, IGFBP5) (see Table 1 for abbreviations).

3.2. Data-mining and network construction

A network of the interactions of genes differentially expressed in GD-HUVEC, and hence in the presence of long term HG in comparison with controls, was built using the MIMI plugin of the freely available software Cytoscape (http://www.cytoscape.org/) [14]. When addressing the pathways analysis, because of the small number of samples analyzed, we firstly verified that results generated with the whole set of genes (including those with a (Log_2) FC of expression between the ± 1 and ± 2 thresholds, see Materials and methods) were significantly not different from that obtained by genes reaching the statistical power of 0.95 (above the ± 2 FC threshold). The search for direct protein–protein and protein–gene interactions produced a very weak relational graph, made of only 9 genes (Fig. 1b, Table 1 for abbreviations and Table 2). Therefore, we thought to expand the network by including "neighboring" genes, factors, molecules or complexes (nodes) that connect differentially expressed genes. These connections were identified by a data-mining approach interrogating public databases with different bioinformatics tools (http://www.genome.jp/kegg/pathway.html, www.genego.com, http://www.sabiosciences.com, http://www.

Table 2
RT-qPCR and primer sequences of arraying-data-mining (d + a) or data-mining (d) genes.
Primer sequences are from 5′ to 3′.

Genes	Origin	Confirmed	RefSeq	Forward primer	Reverse primer
Act	d	nd	NM_031479	ACT ACA GCC AGG GAG TGT GG	GAA AAG TGA GCA GGG AGC TG
ARID5B	d + a	nd	NM_001244638	GGG GAG GGG AGT TGT AAG CA	ATT TGG CGC CAT TCC AGT CG
BDNF	d + a	nd	NM_170734	GTC TCT GGG GAT GCA GAG C	AGC CTT CAT GCA ACC AAA GT
CARD11	d + a	y	NM_032415	CTG GTC GCC TGG AGG AA	CGT TGC ATC TGG ACT TGC
CCND2	d + a	y	NM_001759	AGC TGC TGG CTA AGA TCA CC	ACG GTA CTG CTG CAG GCT AT
CDKN2B	d + a	y	NM_078487	TAC AGG AGT CTC CGT TGG C	GTG AGA GTG GCA GGG TCT G
COL1A1	9 genes	y	NM_000088	AAG AGG AAG GCC AAG TCG AG	CAC ACG TCT CGG TCA TGG TA
COL3A1	9 genes	y	NM_000090	AGG GGA GCT GGC TAC TTC TC	AGG ACT GAC CAA GAT GGG AA
DDR2	9 genes	y	NM_006182	AGG ATC CTG CTC CAC AGA GA	AGG AAC AGC ACC AAG AGC AT
EGF	d	nd	NM_001178131	TCT GCG TGG TGG TGC TTG TC	CCT GCG ACT CCT CAC ATC TC TG
EGFR	d	n	NM_005228	GAG GGT GAG CCA AGG GAG TTT G	GGC AGG TCT TGA CGC AGT GG
F11R	d + a	nd	NM_144502	TCG AGA GGA AAC TGT TGT GC	GAA GAA AAG CCC GAG TAG GC
FBN1	9 genes	y	NM_000138	TCA ATG GAG GAA GGT GTG TG	AAA CAT GGG CCT GTC CTG TA
FBN2	9 genes	y	NM_001999	CCG TGT GCT TGT GTT TAT GG	CTT GGC ACA TCT GGT TGT TG
FGF2	d + a	y	NM_002006	GGA GAA GAG CGA CCC TCA C	AGC CAG GTA ACG GTT AGC AC
FGF2R	d	nd	NM_000141	CCC ACC GCA GGC TGA AGG	CAC GAC CAG GCA GAT GAA ACG
FN1	9 genes	y	NM_002026	CCA TAA AGG GCA ACC AAG AG	ACC TCG GTG TTG TAA GGT GG
FOSL2	d + a	y	NM_005253	GGA ACT TTG ACA CCT CGT CC	TGA GCC AGG CAT ATC TAC CC
FST	9 genes	y	NM_006350	TCT GCC AGT TCA TGG AGG A	TCC TTG CTC AGT TCG GTC TT
FSTL3	d	y	NM_005860	CCA CTC TGG CCT CTG CC	CTG GAG CCA GCA AAC ACC
GH1	d	nd	NM_000515	CCG ACA CCC TCC AAC AGG GA	CCT TGT CCA TGT CCT TCC TG
GHR	d	n	NM_001242399	GGT GAA GGA TGG CGA CTC TG	TGG ATA ACA CTG GGC TG CTG AG
HMOX1	d + a	y	NM_002133	GCC AGC AAC AAA GTG CAA G	GAG TGT AAG GAC CCA TCG GA
ICAM1	d + a	y	NM_000201	TGA TGG GCA GTC AAC AGC TA	AGG GTA AGG TTC TTG CCC AC
IGF1	d	y	NM_000618	TGG ATG CTC TTC AGT TCG TG	TCA TCC ACG ATG CCT GTC T
IGF1R	d	y	NM_000875	GTA CAA CTA CCG CTG CTG GA	TGG CAG CAC TCA TTG TTC TC
IGF2	d	y	NM_000612	GTT CGG TTT GCG ACA CG	AGA AGC ACC AGC ATC GAC TT
IGFBP3	9 genes	y	NM_000598	CTC TGC GTC AAC GCT AGT GC	CGG TCT TCC TCC GAC TCA C
IGFBP5	9 genes	y	NM_000599	GGT TTG CCT CAA CGA AAA GA	GAG TAG GTC TCC TCG GCC AT
IL15	d + a	y	NM_000585	TGT TCC ATC ATG TTC CAT GC	TCC ACG ATG CCT CCT ACA A
INS	d	n	NM_000207	TTC TAC ACA CCC AAG ACC CG	CAA TGC CAC GCT TCT GC
IR	d	n	NM_000208	GTC ATC AAC GGG CAG TTT G	GGT GCA GCC GTG TGA CTT AC
IRS1	d	y	NM_005544	TAT GCC AGC ATC AGT TTC CA	GGA TTT GCT GAG GTC ATT TAG G
IRS2	d	n	NM_003749	ACC TAC GCC AGC ATT GAC TT	CAT CCT GGT GAT AAA GCC AGA
LIPG	d + a	y	NM_006033	GCT GTG GAC TCA ACG ATG TC	GTC AAC AAA GAG GTG GAC GG
MBNL1	d + a	n	NM_021038	AAT GGA CGA GTA ATC GCC TG	CGT TTT TAA ATG TGG GGG TG
mTOR	d	y	NM_004958	CGA GCA TAT GCC AAA GCA CT	TCC GGC TGC TGT AGC TTA TTA
NAMPT	d + a	n	NM_005746	GAG TTC AAC ATC CTC CTG GC	TTC TAC ACA CCC AAG ACC CG
NDRG1	d	n	NM_006096	GTG GAG AAA GGG GAG ACC AT	ACA GCG TGA CGT GAA CAG AG
NEUROD1	d + a	n	NM_002500	GCC CCA GGG TTA TGA GAC TAT	ATC AGC CCA CTC TCG CTG TA
NMI	d	nd	NM_004688	GGG GGT TCG CGT TTC AG	TAT CAG CTT CCA TGA TCC CC
N-MYC	d + a	n	NM_005378	CAC AAG GCC CTC AGT ACC TC	CAC AGT GAC CAC GTC GAT TT
PDGFB	d	n	NM_002608	CAA GAC GGC ACT GAA GGA GAC C	CAA GAC GGC ACT GAA GGA GAC C
PDGFbR	d	y	NM_002609	GCA GCA GTG AGA AGC AAG C	TAG TCC ACC AGG TCT CCG TAG C
PLAT	d + a	y	NM_000930	CTG GAG AGA AAA CCT CTG CG	GCA GAG CCC TCT CTT CAT TG
PLG	d	nd	NM_000301	CTG CCA TCC CCA AAT TAT GT	AGA AGG CCA GCT CCA AAA GT
PSMB8	d + a	n	NM_148919	TCT CCA GAG CTC GCT TTA CC	CAT GGG CCA TCT CAA TCT G
RPS9			NM_001013	CTG CTG ACG CTT GAT GAG AA	CAG CTT CAT CTT GCC CTC AT
SERP1	d	y	NM_000602	ACA ACA GGA GGA GAA ACC CA	AGC TCC TTG TAC AGA TGC CG
SIRT1	d	y	NM_012238	TAC CGA GAT AAC CTT CTG TTC G	GTT CGA GGA TCT GTG CCA AT
SIX2	d + a	y	NM_016932	CAC CAC ACA GGT CAG CAA CT	CGG GTT GTG GCT GTT AGA AT
STAT1	d + a	y	NM_007315	AGG AAG ACC CAA TCC AGA TGT	TGA ATA TTC CCC GAC TGA GC
TFAP2A	d + a	n	NM_003220	ATG CTT TGG AAA TTG ACG GA	ATT GAC CTA CAG TGC CCA GC
TGFB2	d + a	y	NM_003238	ATA GAC ATG CCG CCC TTC TT	CTC CAT TGC TGA GAC GTC AA
TNF-a	d	n	NM_000594	CTG CTG CAC TTT GGA GTG AT	AGA TGA TCT GAC TGC CTG GG
TNFR1	d	n	NM_001065	GGA GTG AGA GGC CAT AGC TG	ATA TTC CCA CCA ACA GCT CC
TNFR2	d	n	NM_001066	CGT CGG ACT GGA GCT CTG	TAT TCT CTG AGC CGG CAT GT
TRADD	d	n	NM_153425	TGC CCA GAC TTT TCT GTT CC	GCC ATT TGA GAC CCA CAG AG
TRAF2	d	y	NM_021138	CCC TTA ACT TGT GAC GGC TG	ATC TGC AAG GGA CTC GAC AC
ZFP36L1	d + a	nd	NM_004926	GTC TGC CAC CAT CTT CGA CT	CTT TCT GTC CAG CAG GCA AC

genecards.org), integrated with interactions with genes recently reported in the literature and not yet annotated in interaction databases. According to this data-mining procedure, we were able to add 83 more nodes to the 9-gene network, Out of these, 23 were genes already included in the Affymetrix chips ("d + a", in Table 2) while the remaining 60 were new nodes (Fig. 2 and Table 1 for abbreviations). The statistical enrichment of GO biological processes of the resulting network, performed by the application of filtering parameters as described above, allowed the clustering in 7 main categories, identical or closely related to those found when considering the 127 genes differentially expressed solely on the basis of the arrays, *i.e.* organ development (GO: 0048513), response to external stimulus (GO: 0009605), immune system process (GO: 0002376), regulation of cellular process (GO: 0050794), embryonic morphogenesis (GO: 0048598), protein metabolic process (GO: 0019538) and enzyme linked receptor protein signaling (GO: 0007167).

3.3. RT-qPCR confirmation of microarray and data-mining

In order to confirm the pivotal role of specific genes in the adaption to HG associated to GD we proceeded to the confirmation by RT-qPCR of 59 genes originating from cDNA arraying-data-mining (9 genes plus 23

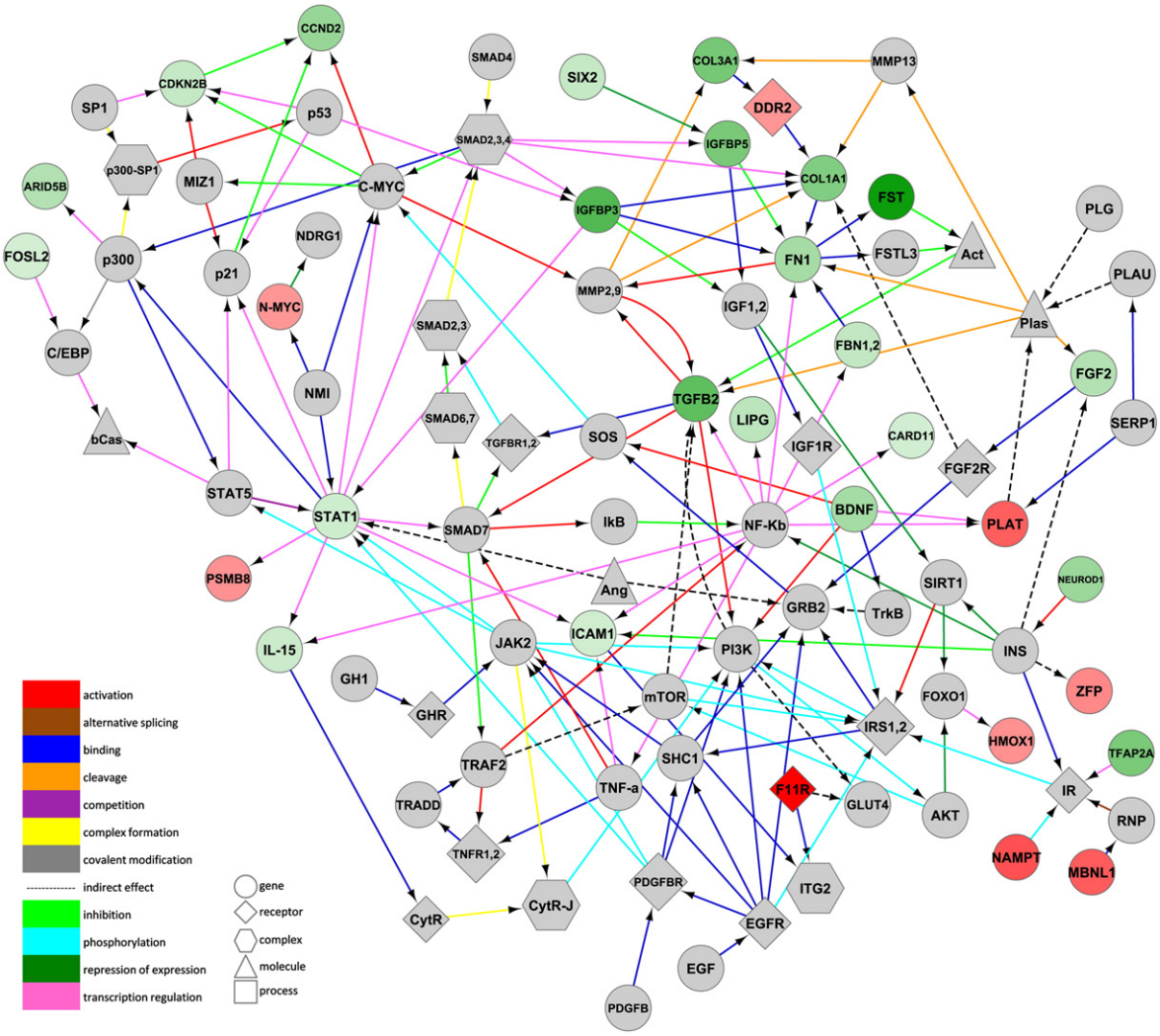

Fig. 2. Network building after data-mining. The 9-gene network of directly connected genes was expanded by data-mining and 83 "neighboring" nodes (genes, factors, molecules or complexes) were included, connecting a total of 32 modulated genes according to microarrays. Green nodes: up-regulated genes; red nodes: down-regulated genes. The intensity of color is proportional to gene regulation level. Gray nodes are nodes inferred by data-mining and lacking array data. Different types of interactions between nodes are colored as indicated.

genes from data-mining, "d + a" in Table 2, column "Origin") or among those obtained solely by data interrogation (27 genes, "d") chosen according to the rationale of being "first-degree neighbors" or because of a known association with diabetes or hyperglycemia. The ribosomal protein RPS9 gene was included for data normalization. The alternative methodology of measurement allowed to confirm the differential expression of 22 out of 32 genes identified by arraying-data-mining (Table 2 "d + a" and "y", Fig. 3), 6 genes were found unchanged with respect to control ("n") and 4 genes were "non-detectable" ("nd") under our analytical conditions. The differential expression of 10, out of 27 genes identified by data-mining and not included in arrays was confirmed (Table 2 "d" and "y", Fig. 3). On the other hand, 11 genes were found not differentially expressed ("n") and six genes were "non-detectable".

3.4. Analysis of methylation status of promoters

Seeking for an epigenetic mechanism able to determine the differential gene expression observed in GD-HUVEC, we analyzed the methylation status of the promoters of 5 genes arbitrarily selected among those significantly affected by HG, namely COL1A1, IGFBP3, IGFBP5, FGF2 and TGFB2 in the individual samples of GD and control subjects. No differences within CpG islands of FGF2 (island 06727), IGFBP5 (island 04169) and COL1A1 (island 22299) were found (data not shown). On the other hand, we found a 44.2 ± 8.9% reduction of the hypermethylated (HM) fraction of genomic DNA in the CpG island 28545 of the TGFB2 promoter of GD-HUVEC correlating with the observed up-regulation of the gene in two out of three GD subjects (strains H46D and H64D, Fig. 5). This effect apparently depends on the emerging intermediately methylated (IM) fraction which was lacking in the third GD subject (H50D, Fig. 5). With respect to IGFBP3, qAMP analysis indicates that the up-regulation of this gene is associated to changes in the methylated fractions within CpG island 28250. However, the effect was not statistically significant (data not shown).

3.5. HG induced up-regulation of TGFB2 gene in Ea.hy926 endothelial cells

In order to corroborate the epigenetic effect of long term HG on TGFB2 observed *in vivo*, we assessed the expression and the methylation status of the same gene in immortalized Ea.hy926 cells cultured in a high glucose concentration, mimicking pathological hyperglycemia (25.5 mM glucose). 24 hour treatment in HG was associated with increased expression of TGFB2 gene (Fig. 6a, unrecovered). The analysis of the methylation of the promoter indicates that TGFB2 up-regulation is associated with a 96.6% reduction of the hypermethylated fraction of genomic DNA

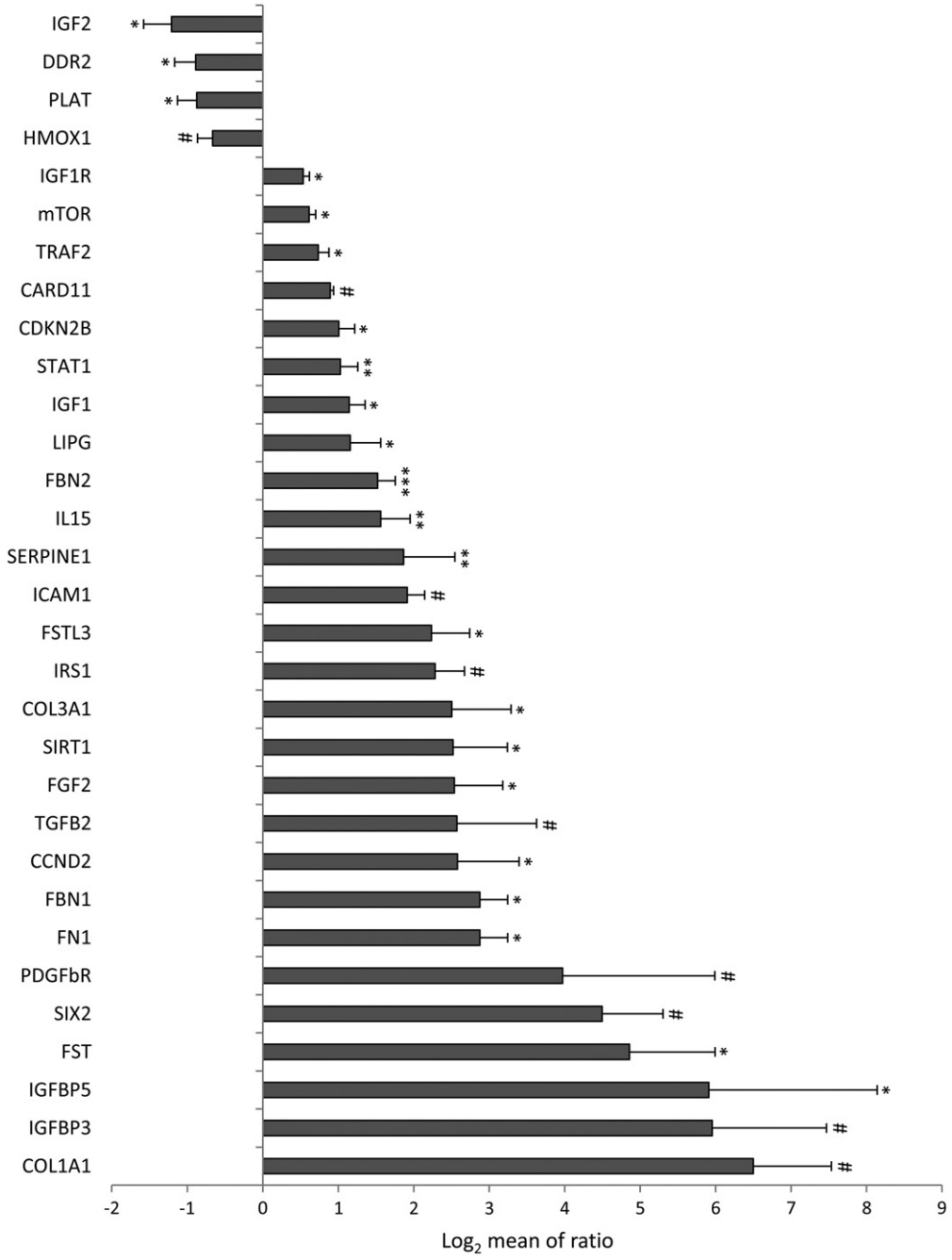

Fig. 3. RT-qPCR summarized. Expression of genes in GD-HUVEC. Results are expressed as geometric mean of Log_2 ratios (values of control HUVEC: 0). Values are means ± SD. Statistical significance was calculated using the unpaired *t* test (*p < 0.05, **p < 0.005, ***p < 0.001, n = 6; #p < 0.05, n = 5).

(Fig. 6b). TGFB2 "glycemic memory" was tested by analyzing the expression of the gene after a 24 hour recovery in normal (5 mM) glucose concentration. Also in this case, the expression of TGFB2 gene significantly increased (Fig. 6a, recovered). At the same time, a 70.8% decrease of the HM fraction was observed in comparison to control (Fig. 6b, recovered), supporting the existence of a methylation-dependent HG-induced memory effect. With respect to IGFBP3 (CpG island 28250), we were unable to quantify DNA methylation because the cell starvation procedure was associated to a complete "switch off" of the expression of the gene, independently of HG (data not shown). However, at the end of 24 hour incubation in non-starving medium after HG treatment, we found a 3.3-fold increase in IGFBP3 gene expression along with a 6.8-fold decrease in promoter methylation (data not shown).

4. Discussion

It has been proposed that HG induces genome-wide epigenetic changes, especially during fetal development, where a profound gene reprogramming occurs [15]. Chronic deregulation of glucose homeostasis can trigger, on the long term, a large number of effects, including diabetes. Within this perspective, HUVEC collected from the umbilical cords of babies delivered by GD mothers have been considered an expedient *ex vivo* model for the study of the molecular consequences of long term, chronic HG. In our study, we have demonstrated that, chronic hyperglycemia *in vivo* is "stabilized" by a specific reprogramming of gene expression in endothelial cells of the infant cords, supporting the existence of a metabolic "glycemic memory", *i.e.*

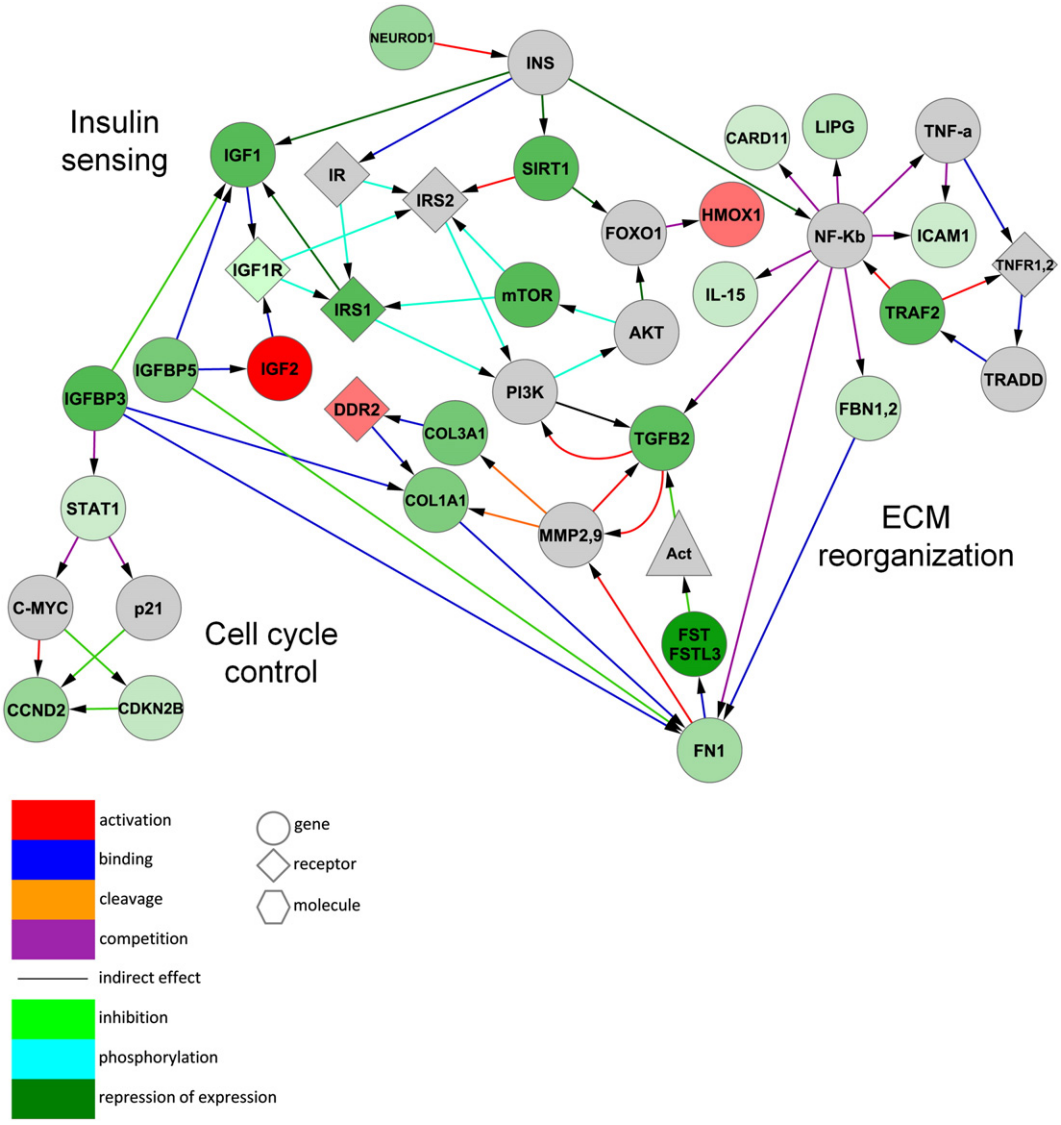

Fig. 4. Summary of GD-HUVEC major changes. Interaction network between genes, receptors and molecules obtained by RT-qPCR confirmation of data-mining and microarray findings in GD-HUVEC. Focus is on genes involved in insulin sensing, ECM reorganization and cell cycle. The intensity of color is proportional to gene regulation level. Gray nodes are nodes inferred by data-mining and lacking array data. Different types of interactions between nodes are colored as indicated.

a glucose-dependent epigenetic reprogramming of gene expression [16] (and references cited herein).

mRNA of GD-HUVEC cultures were subjected to transcriptome analysis utilizing a Affymetrix 3′ microarray platform. 127 genes were found differentially modulated in GD endothelial cells in comparison to controls. The reconstruction of the network of direct interactions of modulated genes allowed the construction of a very low relational graph (Fig. 1b). The bolstering of the network analysis, by means of a data-mining approach, allowed the inclusion of 83 more nodes in the 9-gene graph (Fig. 2), inclusive of 23 genes already identified by arrays. Among the identified genes, a total of 59 genes were arbitrarily selected for RT-qPCR quantification of gene expression (Fig. 3), 32 included in chips and 27 identified by data-mining alone (Table 2). The modulation of 32 genes was confirmed ("y"), 22 from arraying-data-mining ("d + a") and 10 from data-mining ("d"), respectively (Fig. 4 summarizes GD-HUVEC major changes).

Hereinafter, gene expression profile identified by our analyses grouped by different functional categories will be described and discussed, mainly addressing the differential expression of genes displaying a (Log_2) FC above the ± 2 threshold (0.95 of power), in order to ensure higher statistical significance.

4.1. Growth factors and proteins linked to insulin sensing (IGFBP3, IGFBP5, IRS1, SIRT1, mTOR)

The increased expression of insulin-like growth factor binding proteins IGFBP3 and IGFBP5 in GD-HUVEC, as detected with microarrays (two of the 9-gene network genes, Fig. 1b) and further confirmed by RT-qPCR (Table 2, Figs. 3 and 4) is consistent with previous observations on pregnancies complicated with hyperglycemia [17] and GD [18]. GD women also show increased protein levels of insulin receptor substrate-1 (IRS1) in the placenta [19]. The gene, identified as a "neighbor" in our data-mining analysis, was found up-regulated in GD-HUVEC by RT-qPCR (Fig. 3). This observation suggests the existence of an HG-dependent epigenetic regulation mechanism involving the receptor. This hypothesis is supported by others who previously reported an HG-dependent increase of insulin-sensitiveness in human aortic endothelial cells [20].

SIRT1, a NAD-dependent protein deacetylase that links the regulation of gene expression to the energetic status of the cell by "sensing" glucose availability and metabolism [21] is another "neighbor" of IGFBPs identified by data-mining (Fig. 2). By means of RT-qPCR, we assessed an up-regulation of SIRT1 in GD-HUVEC (Figs. 3 and 4). This observation apparently mismatches the down-regulation induced by glucose reported by others [22]. On the other hand, it is possible to hypothesize that SIRT1 acts by "sensing" the environment shift from maternal HG to the *in vitro* normal glucose. The hypothesis of a HG-dependent regulation of SIRT1 expression is consistent with the epigenetic properties of deacetylases. A similar hypothesis has been already proposed for mTOR, as a placental sensor of maternal nutrients availability, hence regulating nutrient transport and fetal growth [23]. Notably, the up-regulation of SIRT1 matches with mTOR up-regulation (Figs. 3 and 4). This candidate role of mTOR is supported by data from pregnancies characterized by intrauterine growth restriction (a situation opposite to that occurring in GD) in which mTOR was found reduced at the protein level. mTOR also links the insulin cascade to the PI3K–AKT kinase [24], and the PI3K gene was reported down-regulated in HUVEC temporarily treated with pharmacologic doses of insulin [25]. The lack of PI3K mRNA modulation in our model could rely on the different and more physiological condition of GD-HUVEC cells. On the other hand, at the protein level, AKT phosphorylation can be triggered by SIRT1–mTOR signaling, and this regulation triggers the phosphorylation of AKT (and FOXO1) leading to a decreased transcription of gluconeogenic genes [26] and increased glucose uptake due to the translocation of the glucose transporter 4 (GLUT4) to the plasma membrane [27]. All the above mentioned responses result in an increased conversion of glucose to glycogen, a situation similar to that taking place *in vitro* in GD-HUVEC.

4.2. Factors involved in ECM reorganization (TGFB2, FBN1, FBN2, COL1A1, COL3A1, DDR2, FN1, FST, FSTL3, CARD11, LIPG, ICAM1)

We found a strong up-regulation of transforming growth factor β 2 (TGFB2) in two out of three samples of GD-HUVEC (strains H46D and H64D). This condition was associated to decreased hypermethylation of the promoter (Fig. 5). A different methylation pattern was found in the third strain (H50D) that showed a lower up-regulation of TGFB2 in comparison to the other two. The direct correlation between promoter methylation status and expression level supports an epigenetic regulation mechanism, and also indicates a complex regulation mechanism that surely needs further investigations to be fully elucidated. However, our observation is corroborated by the *in vitro* confirmation in Ea.hy926 cells, and is the first report describing a glucose-dependent epigenetic mechanism regulating TGFB2 gene expression by a differential methylation of its promoter.

TGFBs are secreted cytokine involved in several cellular responses and have crucial roles during development but also in the homeostasis of most human tissues. Disruption of TGFB homeostasis affects different cellular functions, from proliferation to differentiation, eventually leading to vascular remodeling and tumor formation [28]. In non-tumor cells, upon ligand binding, TGFB receptors dimerize and activate a signaling cascade involving SMAD proteins and finally the transcription of TGFB dependent genes [29]. In cancer cells, TGFB pro-metastatic and pro-inflammatory effects are regulated *via* nuclear factor kappa B (NF-κB) [30]. It is possible to hypothesize that the effects of hyperglycemia in GD-HUVEC could involve NF-κB-dependent activation of TGFB2. This hypothesis is supported by several evidences, namely: i) a specific up-regulation of TGFB2 has been recently found associated to hyperglycemia in retinal pericytes [31]; ii) a putative NF-κB site within TGFB2 promoter has been identified by sequence analysis of TGFB2 regulatory regions [32]; iii) TGFB2 has been reported to be responsible for NF-κB activation [33], and iv) transient HG has been found to induce the expression of the gene coding the p65 subunit of NF-κB both *in vivo* in mice, and *in vitro*, in aortic endothelial cells [34]. In the latter study, the effect of HG on p65 expression was persistent after the restoration

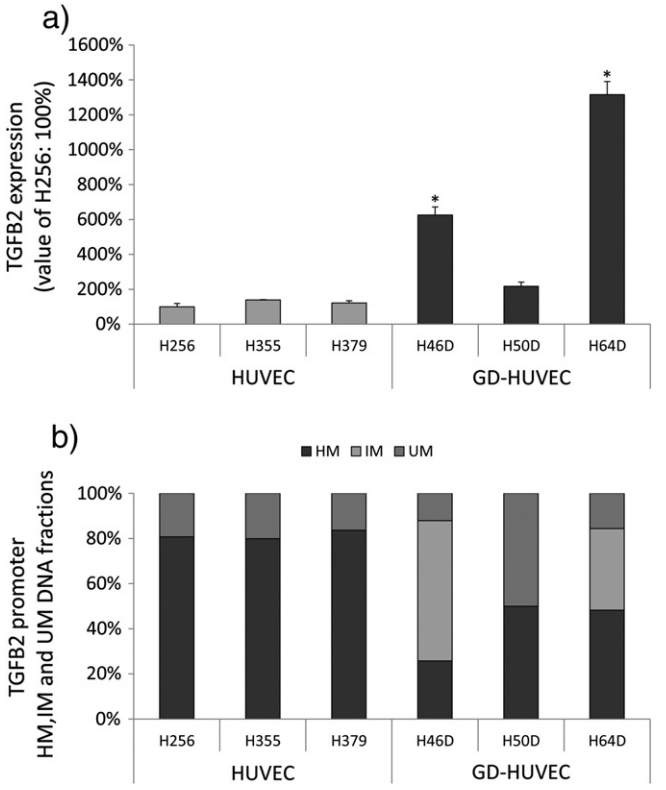

Fig. 5. Expression and promoter methylation of TGFB2 in GD-HUVEC. (a) Expression of TGFB2 in GD-HUVEC strains (H46D, H50D, H64D) and in control HUVEC strains (H256, H355, H379). Results are expressed as percent values of H355, H379, H46D, H50D and H64D expression with respect to that of H256, arbitrarily set equal to 100. Values are means ± SD from qPCR run in technical triplicates. H46D and H64D GD-HUVEC samples displayed differential expression compared to HUVEC controls by unpaired *t* test at $p < 0.05$ level. (b) TGFB2 promoter methylated fractions within CpG island 28545 in the same HUVEC strains as in Fig. 5a quantified by qAMP. Results are expressed as percent values of H256, H355, H379, H46D, H50D and H64D hypermethylated (HM), unmethylated (UM) and intermediately methylated (IM) DNA fractions. Values are means from qAMP run in technical triplicates.

of normoglycemia and depended on increased methylation of the histone H3K4 by the methyltransferase Set7, demonstrating that HG is able to trigger an epigenetic regulatory mechanism [34]. According to these reports, cancer cell lines expressing high levels of secreted TGFB2 also show a constitutive activation of NF-κB, considered essential for the escape of tumor cells from apoptosis. Finally, the hypothesis of a NF-κB-dependent activation of TGFB2 in GD-HUVEC is supported by the up-regulation of the expression of genes located both downstream and upstream to NF-κB, namely: ICAM1, CARD11, LIPG, IL15 and TRAF2 [35] (Figs. 3 and 4).

The involvement of NF-κB is further supported by the strong up-regulation of Fibronectin (FN1), an ECM glycoprotein (Figs. 1b and 4). FN1 induces the activation of MMP2 and MMP9, triggering the proteolytic process required for TGFB release and activation [36]. Similarly, in colon cancer cells, the activation of MMP2 by FN1 depends on NF-κB [37]. Moreover, the up-regulation of FN1 has also been reported by others in endothelial cells exposed to HG [38]. Notably, FN1 up-regulation was shown to persist in cultured cells for several cell divisions after the restoration of normoglycemia corroborating the hypothesis of a "phenomenon with a memory" [39]. Increased expression of FN1 was also observed in rat embryos from diabetic mothers [40], a condition analogous to GD. More recently, HG has been shown to be associated to an increase of the binding of the epigenetically regulated transcriptional coactivator p300 to the FN1 promoter in the same experimental model (HUVEC) [41].

Downstream to FN1, GD-HUVEC displayed a high expression of Follistatin (FST) and FST like-3 (FSTL3) (Fig. 4) according to array analysis (Fig. 1b) and by data-mining (Fig. 2), respectively. These proteins are antagonists of TGFB2 ligands, like Activin (Fig. 4), which modulate glucose homeostasis, islet function and contribute to the regulation of body composition [42]. Maternal and placental concentrations of FSTL3 in GD women have been found reduced in comparison with normal pregnant women, indicating that FSTL3 is implicated in GD [43]. Also in this case, more studies are mandatory for a better understanding of the occurrence of opposite effects on FSTL3 expression and about the role of FST in hyperglycemia. Similar to the up-regulation of the glucose sensor SIRT1, the up-regulation of FSTL3 in GD could be interpreted as the consequence of a shift from a hyper- to a normoglycemic milieu in culture medium after the isolation of HUVEC from umbilical cords.

As mentioned above, TGFBs induce the accumulation of collagen proteins COL1A1 and COL3A1 (collagen, type I and III, alpha 1), that were found up-regulated in GD-HUVEC, according to both array analysis (Fig. 1b) and RT-qPCR (Fig. 3), together with FBN (Fibrillins 1 and 2). Both FBNs and COL1A1 and COL3A1 have been recognized to be epigenetically regulated [44,45]. However, no differential methylation of the CpG 22299 island of COL1A1 promoter was found in the present study, suggesting that other islands sensitive to methylation are possibly involved. Even though COL3A1 specifically activates DDR2 (Fig. 4), a tyrosine kinase involved in ECM remodeling [46] through MMP2 [47] we observed a down-regulation of this kinase by arrays (Fig. 1b) and by RT-qPCR (Fig. 3). We can speculate that the down-regulation of DDR2 is the consequence of a negative feedback operated in GD-HUVEC by the protein on the messenger, as already proposed for dermal fibroblasts [48].

Centrally in our study, the up-regulation of TGFB2 in the presence of a long term HG was fully confirmed in a different endothelial cell model, the Ea.hy926 cells (Fig. 6). Importantly, the up-regulation was not reverted by the return to normoglycemic conditions and it was associated with a reduction of the hypermethylated fraction of genomic DNA within TGFB2 gene promoter (Fig. 6). Also in this case more specific studies are needed in order to verify the occurrence of NF-κB activation as the result of epigenetic changes induced by HG.

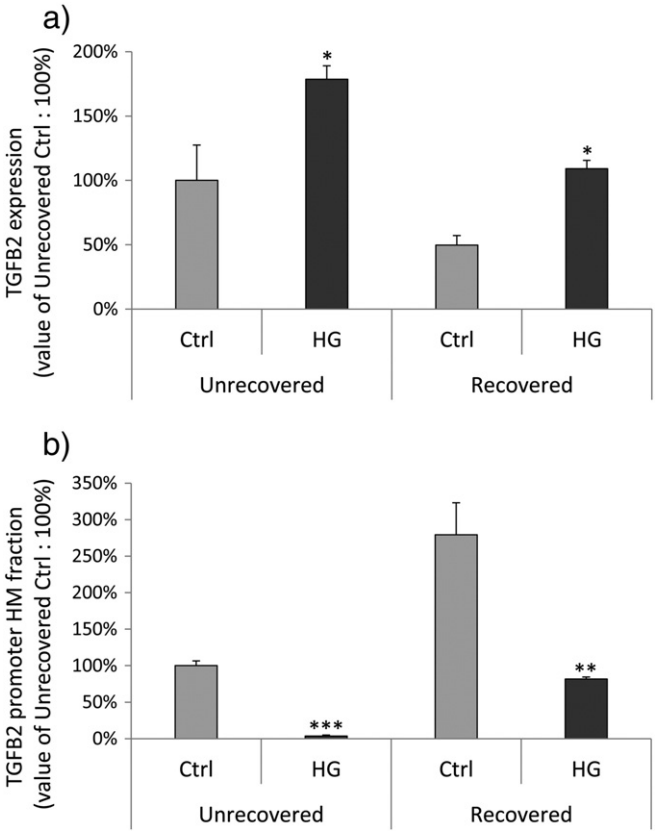

Fig. 6. Expression and promoter methylation of TGFB2 in Ea.hy926. Ea.hy926 cells were treated for 24 h with 25.5 mM glucose (unrecovered) or for 24 h followed by a 24 hour recovery in normal glucose (recovered) in order to test the "glycemic memory". (a) Expression of TGFB2 by RT-qPCR. (b) Quantification of the HM DNA fraction within CpG island 28545 of TGFB2 promoter qAMP. UM and IM fractions were omitted because these were found equal to 0. Gene expression and promoter HM are expressed as percent values with respect to unrecovered control cells, arbitrarily set equal to 100. Values are means ± SD from three independent experiments. Statistical significance was calculated using the unpaired *t* test (*$p < 0.05$, **$p < 0.005$, ***$p < 0.001$).

4.3. Non-insulin growth factors (FGF2, PDGFbR)

GD is characterized by macrosomia. In agreement with this phenotype, high concentrations of several non-insulin associated growth factors and receptors have been observed in the serum and in the placenta of GD women and in their offspring, namely: GH1, EGF, FGF2, VEGF, ET-1 (EDN1), PDGFB, GHR, EGFR and PDGFbR [49,50] (and references cited herein). In our study no differences were found in PDGFB, GHR and EGFR expression associated to GD-HG, while we detected a significant up-regulation of FGF2 and PDGFbR (Fig. 3). The increase of FGF2 expression observed in our study is consistent with previously published data showing that HG is associated with an increase of this membrane-associated protein in endothelial cell basement, in a time-dependent fashion and persistently, even after the recovery to normoglycemia [51]. We found no differences in the methylation of FGF2 promoter (CpG island 06727) in GD-HUVEC in comparison to controls (data not shown). Inaba and coworkers reported that HG increases the expression of PDGFbR in human capillary endothelial cells [52] and in rat vascular smooth muscle cells [53]. The up-regulation of PDGF receptor in GD-HUVEC is likely to be due to reduced levels of the growth factor or to a cellular set up mimicking the effect of a previous hyperglycemic condition that remained fixed, possibly by an epigenetic mechanism. In agreement with this hypothesis, the demethylation of a specific region of PDGFbR promoter has been recently correlated to the up-regulation of PDGFbR expression during the differentiation of human embryonic stem into fibroblasts [54].

4.4. Cell cycle genes (CCND2, CDKN2B)

By means of population studies, the epigenetically regulated cyclin-dependent kinase inhibitor 2B (CDKN2B; p15INK4b) [55] has been recently linked to T2D in several European and Asiatic populations [56] (and references cited herein). Moreover, using antisense oligonucleotides, Chen et al. revealed a role of the gene in HG-induced endothelial cell growth inhibition [57]. Even if more experiments are required for the comprehension of the role of CDKN2B (and similarly cyclin D2, CCND2) in T2D, the observed up-regulation in GD-HUVEC (Fig. 3) supports the idea of an epigenetical regulation by chronic HG during gestational diabetes.

4.5. Final considerations

Even if a small number of samples were analyzed, data presented here, supported by strong statistical analysis, provide a set of novel information and an original database addressing the effects of long term hyperglycemia on fetal tissues, potentially contributing to long term health consequences. Moreover, we have generated a background that contributes to a better understanding of the molecular mechanisms responsible for the specific fixation of HG phenotype in the genome during fetal development. In particular, we focused on the existence of an epigenetic mechanism regulating TGFB2 expression by glucose, confirmed *in vitro* by HG treatment on Ea.hy926 cells.

Our study highlights the candidate role of proteins linked to insulin sensing and ECM reorganization (Fig. 4). We suggest that the activation of the insulin signaling pathway by hyperglycemia could depend upstream on NF-κB, SIRT1 and mTOR and, downstream, on an epigenetic modulation of TGFB2 through a reduced hypermethylation of the promoter.

Our data also confirm that GD-HUVEC are an expedient model for the study of the molecular mechanisms involved in endothelial dysfunction resulting from HG occurring during gestational diabetes. In fact, gene expression profile observed in GD-HUVEC recapitulates almost all findings that have been reported in GD and in endothelial cells challenged with HG. However, the HG-dependent mechanism responsible for the observed epigenetic modification of TGFB2 expression yet remains to be elucidated.

Financial disclosure

This research was supported by grants from the Ministero delle Politiche Agricole Alimentari e Forestali (projects "NUME" and "MEDITO"). The funders had no role in study design, data collection and analysis, decision to publish, or preparation of the manuscript.

Acknowledgments

The authors wish to acknowledge Sara Di Silvestre and Pamela Di Tomo for their technical support for cell culture.

References

[1] S.M. Baumgartner-Parzer, L. Wagner, M. Pettermann, J. Grillari, A. Gessl, W. Waldhausl, High-glucose-triggered apoptosis in cultured endothelial cells, Diabetes 44 (1995) 1323–1327.
[2] G.C. Koh, S.J. Peacock, T. van der Poll, W.J. Wiersinga, The impact of diabetes on the pathogenesis of sepsis, Eur. J. Clin. Microbiol. Infect. Dis. 31 (2012) 379–388.
[3] C. Nielson, T. Lange, Blood glucose and heart failure in nondiabetic patients, Diabetes Care 28 (2005) 607–611.
[4] T.A. Buchanan, A.H. Xiang, Gestational diabetes mellitus, J. Clin. Invest. 115 (2005) 485–491.
[5] E.M. Wendland, M.R. Torloni, M. Falavigna, J. Trujillo, M.A. Dode, M.A. Campos, B.B. Duncan, M.I. Schmidt, Gestational diabetes and pregnancy outcomes — a systematic review of the World Health Organization (WHO) and the International Association of Diabetes in Pregnancy Study Groups (IADPSG) diagnostic criteria, BMC Pregnancy Childbirth 12 (2012).
[6] I. Lambrinoudaki, S.A. Vlachou, G. Creatsas, Genetics in gestational diabetes mellitus: association with incidence, severity, pregnancy outcome and response to treatment, Curr. Diab. Rev. 6 (2010) 393–399.
[7] J. Robitaille, A.M. Grant, The genetics of gestational diabetes mellitus: evidence for relationship with type 2 diabetes mellitus, Genet. Med. 10 (2008) 240–250.
[8] M.E. Cooper, A. El-Osta, Epigenetics: mechanisms and implications for diabetic complications, Circ. Res. 107 (2010) 1403–1413.
[9] M. Federici, A. Pandolfi, E.A. De Filippis, G. Pellegrini, R. Menghini, D. Lauro, M. Cardellini, M. Romano, G. Sesti, R. Lauro, A. Consoli, G972R IRS-1 variant impairs insulin regulation of endothelial nitric oxide synthase in cultured human endothelial cells, Circulation 109 (2004) 399–405.
[10] C.J.S. Edgell, C.C. McDonald, J.B. Graham, Permanent cell line expressing human factor VIII-related antigen established by hybridization, Proc. Natl. Acad. Sci. U. S. A. 80 (1983) 3734–3737.
[11] W. Qiu, M.L.T. Lee, G.A. Whitmore, Sample size and power calculation in microarray studies, R package version 1.26.0, 2006.
[12] C.C. Oakes, S. Salle, J.M. Trasler, B. Robaire, Restriction digestion and real-time PCR (qAMP) DNA methylation, in: J. Tost (Ed.), Humana Press, 2009, pp. 271–280.
[13] R. Edgar, M. Domrachev, A.E. Lash, Gene Expression Omnibus: NCBI gene expression and hybridization array data repository, Nucleic Acids Res. 30 (2002) 207–210.
[14] J. Gao, A.S. Ade, V.G. Tarcea, T.E. Weymouth, B.R. Mirel, H.V. Jagadish, D.J. States, Integrating and annotating the interactome using the MiMI plugin for cytoscape, Bioinformatics 25 (2009) 137–138.
[15] A. Chmurzynska, Fetal programming: link between early nutrition, DNA methylation, and complex diseases, Nutr. Rev. 68 (2010) 87–98.
[16] A. El-Osta, Glycemic memory, Curr. Opin. Lipidol. 23 (2012) 24–29.
[17] U. Hiden, E. Glitzner, M. Hartmann, G. Desoye, Insulin and the IGF system in the human placenta of normal and diabetic pregnancies, J. Anat. 215 (2009) 60–68.
[18] S.C. Cwyfan Hughes, M.R. Johnson, G. Heinrich, J.M.P. Holly, Could abnormalities in insulin-like growth factors and their binding proteins during pregnancy result in gestational diabetes? J. Endocrinol. 147 (1995) 517–524.
[19] M. Colomiere, M. Permezel, C. Riley, G. Desoye, M. Lappas, Defective insulin signaling in placenta from pregnancies complicated by gestational diabetes mellitus, Eur. J. Endocrinol. 160 (2009) 567–578.
[20] A.R. Gosmanov, F.B. Stentz, A.E. Kitabchi, De novo emergence of insulin-stimulated glucose uptake in human aortic endothelial cells incubated with high glucose, Am. J. Physiol. Endocrinol. Metab. 290 (2006) E516–E522.
[21] Z. Cheng, Y. Tseng, M.F. White, Insulin signaling meets mitochondria in metabolism, Trends Endocrinol. Metab. 21 (2010) 589–598.
[22] M. Orimo, T. Minamino, H. Miyauchi, K. Tateno, S. Okada, I. Komuro, Protective role of SIRT1 in diabetic vascular dysfunction, Arterioscler. Thromb. Vasc. Biol. 29 (2009) 889–894.
[23] S. Roos, N. Jansson, I. Palmberg, K. Säljö, T.L. Powell, T. Jansson, Mammalian target of rapamycin in the human placenta regulates leucine transport and is down-regulated in restricted fetal growth, J. Physiol. 582 (2007) 449–459.
[24] J. Li, K. DeFea, R.A. Roth, Modulation of insulin receptor substrate-1 tyrosine phosphorylation by an Akt/phosphatidylinositol 3-kinase pathway, J. Biol. Chem. 274 (1999) 9351–9356.
[25] B. Di Camillo, T. Sanavia, E. Iori, V. Bronte, E. Roncaglia, A. Maran, A. Avogaro, G. Toffolo, C. Cobelli, The transcriptional response in human umbilical vein endothelial cells exposed to insulin: a dynamic gene expression approach, PLoS One 5 (2010) e14390.
[26] R.H. Wang, H.S. Kim, C. Xiao, X. Xu, O. Gavrilova, C.X. Deng, Hepatic Sirt1 deficiency in mice impairs mTorc2/Akt signaling and results in hyperglycemia, oxidative damage, and insulin resistance, J. Clin. Invest. 121 (2011) 4477–4490.
[27] M.R. Calera, C. Martinez, H. Liu, A.K. El Jack, M.J. Birnbaum, P.F. Pilch, Insulin increases the association of Akt-2 with Glut4-containing vesicles, J. Biol. Chem. 273 (1998) 7201–7204.
[28] E. Pardali, M.J. Goumans, P. ten Dijke, Signaling by members of the TGF-beta family in vascular morphogenesis and disease, Trends Cell Biol. 20 (2010) 556–567.
[29] L. Kubiczkova, L. Sedlarikova, R. Hajek, S. Sevcikova, TGF-beta — an excellent servant but a bad master, J. Transl. Med. 10 (2012) 183.
[30] G. Monteleone, J. Mann, I. Monteleone, P. Vavassori, R. Bremner, M. Fantini, G. Del Vecchio Blanco, R. Tersigni, L. Alessandroni, D. Mann, F. Pallone, T.T. MacDonald, A failure of transforming growth factor-beta1 negative regulation maintains sustained NF-kappaB activation in gut inflammation, J. Biol. Chem. 279 (2004) 3925–3932.
[31] E.K. Vidro, S. Gee, R. Unda, J.X. Ma, A. Tsin, Glucose and TGFβ2 modulate the viability of cultured human retinal pericytes and their VEGF release, Curr. Eye Res. 33 (2008) 984–993.
[32] U. Malipiero, M. Holler, U. Werner, A. Fontana, Sequence analysis of the promoter region of the glioblastoma derived T cell suppressor factor/transforming growth factor (TGF)-β2 gene reveals striking differences to the TGF-β1 and -β3 genes, Biochem. Biophys. Res. Commun. 171 (1990) 1145–1151.
[33] T. Lu, L.G. Burdelya, S.M. Swiatkowski, A.D. Boiko, P.H. Howe, G.R. Stark, A.V. Gudkov, Secreted transforming growth factor β2 activates NF-κB, blocks apoptosis, and is essential for the survival of some tumor cells, Proc. Natl. Acad. Sci. U. S. A. 101 (2004) 7112–7117.
[34] A. El-Osta, D. Brasacchio, D. Yao, A. Pocai, P.L. Jones, R.G. Roeder, M.E. Cooper, M. Brownlee, Transient high glucose causes persistent epigenetic changes and altered gene expression during subsequent normoglycemia, J. Exp. Med. 205 (2008) 2409–2417.
[35] D. Ait-Ali, V. Turquier, Y. Tanguy, E. Thouënnon, H. Ghzili, L. Mounien, C. Derambure, S. Jégou, J.P. Salier, H. Vaudry, L.E. Eiden, Y. Anouar, Tumor necrosis factor (TNF)-α persistently activates nuclear factor-κB signaling through the type 2 TNF receptor in chromaffin cells: implications for long-term regulation of neuropeptide gene expression in inflammation, Endocrinology 149 (2008) 2840–2852.
[36] D.B. Rifkin, Latent transforming growth factor-β (TGF-β) binding proteins: orchestrators of TGF-β availability, J. Biol. Chem. 280 (2005) 7409–7412.
[37] H. Ito, M. Duxbury, E. Benoit, R.S. Farivar, J. Gardner-Thorpe, M.J. Zinner, S.W. Ashley, E.E. Whang, Fibronectin-induced COX-2 mediates MMP-2 expression and invasiveness of rhabdomyosarcoma, Biochem. Biophys. Res. Commun. 318 (2004) 594–600.
[38] E. Cagliero, M. Maiello, D. Boeri, S. Roy, M. Lorenzi, Increased expression of basement membrane components in human endothelial cells cultured in high glucose, J. Clin. Invest. 82 (1988) 735–738.
[39] S. Roy, R. Sala, E. Cagliero, M. Lorenzi, Overexpression of fibronectin induced by diabetes or high glucose: phenomenon with a memory, Proc. Natl. Acad. Sci. U. S. A. 87 (1990) 404–408.
[40] E. Cagliero, H. Forsberg, R. Sala, M. Lorenzi, U.J. Eriksson, Maternal diabetes induces increased expression of extracellular matrix components in rat embryos, Diabetes 42 (1993) 975–980.
[41] S. Chen, B. Feng, B. George, R. Chakrabarti, M. Chen, S. Chakrabarti, Transcriptional coactivator p300 regulates glucose-induced gene expression in endothelial cells, Am. J. Physiol. Endocrinol. Metab. 298 (2010) E127–E137.
[42] M.L. Brown, L. Bonomi, N. Ungerleider, J. Zina, F. Kimura, A. Mukherjee, Y. Sidis, A. Schneyer, Follistatin and follistatin like-3 differentially regulate adiposity and glucose homeostasis, Obesity (Silver Spring) 19 (2011) 1940–1949.
[43] D. Hu, T. Tian, J. Guo, H. Wang, D. Chen, M. Dong, Decreased maternal and placental concentrations of follistatin-like 3 in gestational diabetes, Clin. Chim. Acta 413 (2012) 533–536.
[44] R. Cortese, O. Hartmann, K. Berlin, F. Eckhardt, Correlative gene expression and DNA methylation profiling in lung development nominate new biomarkers in lung cancer, Int. J. Biochem. Cell Biol. 40 (2008) 1494–1508.
[45] A.B. Gaikwad, J. Gupta, K. Tikoo, Epigenetic changes and alteration of Fbn1and Col3A1gene expression under hyperglycaemic and hyperinsulinaemic conditions, Biochem. J. 432 (2010) 333–341.
[46] W. Vogel, G.D. Gish, F. Alves, T. Pawson, The discoidin domain receptor tyrosine kinases are activated by collagen, Mol. Cell 1 (1997) 13–23.
[47] N. Ferri, N.O. Carragher, E.W. Raines, Role of discoidin domain receptors 1 and 2 in human smooth muscle cell-mediated collagen remodeling: potential implications in atherosclerosis and lymphangioleiomyomatosis, Am. J. Pathol. 164 (2004) 1575–1585.

[48] K. Makino, M. Jinnin, J. Aoi, A. Hirano, I. Kajihara, T. Makino, K. Sakai, S. Fukushima, Y. Inoue, H. Ihn, Discoidin domain receptor 2-microRNA 196a-mediated negative feedback against excess type I collagen expression is impaired in scleroderma dermal fibroblasts, J. Invest. Dermatol. 133 (2012) 110–119.
[49] O. Grissa, A. Yessoufou, I. Mrisak, A. Hichami, D. Amoussou-Guenou, A. Grissa, F. Djrolo, K. Moutairou, A. Miled, H. Khairi, M. Zaouali, I. Bougmiza, A. Zbidi, Z. Tabka, N.A. Khan, Growth factor concentrations and their placental mRNA expression are modulated in gestational diabetes mellitus: possible interactions with macrosomia, BMC Pregnancy Childbirth 10 (2010).
[50] M.C. Lygnos, K.I. Pappa, H.A. Papadaki, C. Relakis, E. Koumantakis, N.P. Anagnou, G.D. Eliopoulos, Changes in maternal plasma levels of VEGF, bFGF, TGF-β1, ET-1 and sKL during uncomplicated pregnancy, hypertensive pregnancy and gestational diabetes, In Vivo 20 (2006) 157–164.
[51] A.S. Morss, E.R. Edelman, Glucose modulates basement membrane fibroblast growth factor-2 via alterations in endothelial cell permeability, J. Biol. Chem. 282 (2007) 14635–14644.
[52] T. Inaba, S. Ishibashi, T. Gotoda, M. Kawamura, N. Morino, Y. Nojima, M. Kawakami, Y. Yazaki, N. Yamada, Enhanced expression of platelet-derived growth factor-β receptor by high glucose: involvement of platelet-derived growth factor in diabetic angiopathy, Diabetes 45 (1996) 507–512.
[53] H. Shimizu, Y. Nakagawa, C. Murakami, N. Aoki, S. Kim-Mitsuyama, H. Miyazaki, Protein tyrosine phosphatase PTPεM negatively regulates PDGF β-receptor signaling induced by high glucose and PDGF in vascular smooth muscle cells, Am. J. Physiol. Cell Physiol. 299 (2010) C1144–C1152.
[54] K.J. Hewitt, Y. Shamis, E. Knight, A. Smith, A. Maione, A. Alt-Holland, S.D. Sheridan, S.J. Haggarty, J.A. Garlick, PDGFRβ expression and function in fibroblasts derived from pluripotent cells is linked to DNA demethylation, J. Cell Sci. 125 (2012) 2276–2287.
[55] S. Kusy, C.J. Larsen, J. Roche, p14ARF, p15INK4b and p16INK4a methylation status in chronic myelogenous leukemia, Leuk. Lymphoma 45 (2004) 1989–1994.
[56] M.L. Hribal, I. Presta, T. Procopio, M.A. Marini, A. Stančáková, J. Kuusisto, F. Andreozzi, A. Hammarstedt, P.A. Jansson, N. Grarup, T. Hansen, M. Walker, N. Stefan, A. Fritsche, H.U. Häring, O. Pedersen, U. Smith, M. Laakso, G. Sesti, Glucose tolerance, insulin sensitivity and insulin release in European non-diabetic carriers of a polymorphism upstream of CDKN2A and CDKN2B, Diabetologia 54 (2011) 795–802.
[57] Y.H. Chen, J.Y. Guh, T.D. Chuang, H.C. Chen, S.J. Chiou, J.S. Huang, Y.L. Yang, L.Y. Chuang, High glucose decreases endothelial cell proliferation via the extracellular signal regulated kinase/p15INK4b pathway, Arch. Biochem. Biophys. 465 (2007) 164–171